Plant Physiology Preview. Published on April 17, 2013, as DOI:10.1104/pp.112.212837

Running head: ASF1 proteins in cell cycle and UV responses

Corresponding author: Paula Casati
Centro de estudios Fotosintéticos y Bioquímicos (CEFOBI)
Suipacha 531
2000 Rosario, Argentina
Tel: + (54) 341 4371955
e-mail: casati@cefobi-conicet.gov.ar
Journal research area: Environmental Stress and Adaptation

ASF1 Proteins are Involved in UV-induced DNA Damage Repair and are Cell Cycle Regulated by E2F Transcription Factors in *Arabidopsis thaliana*

Luciana D. Lario[1], Elena Ramirez-Parra[2], Crisanto Gutierrez[3], Claudia P. Spampinato[1] and Paula Casati[1,*]

[1] Centro de Estudios Fotosintéticos y Bioquímicos (CEFOBI), Universidad Nacional de Rosario, Suipacha 531, 2000 Rosario, Argentina.

[2] Centro de Biotecnología y Genómica de Plantas, Instituto Nacional de Investigación y Tecnología Agraria y Alimentaria, Universidad Politécnica de Madrid, Campus de Montegancedo, 28223 Pozuelo de Alarcón, Madrid, Spain

[3] Centro de Biología Molecular 'Severo Ochoa', Consejo Superior de Investigaciones Científicas, Universidad Autónoma de Madrid, Cantoblanco, 28049 Madrid, Spain.

Financial Source: This research was supported by FONCyT grants PICT 2007-00711 and 2010-00105 to P.C, grants from FONCYT (PICT 2010-0458), CONICET (PIP 0018) and UNR (BIO 221) to C.P.S and grants BFU2009-9783 and CSD2007-00057-B (Ministry of Science and Innovation) to C.G, by an institutional grant from Fundación Ramón Areces to CBM. C.P.S. and P.C. are members of the Researcher Career of the Consejo Nacional de Investigaciones Científicas y Técnicas (CONICET), and L.D.L. is a fellow from this Institution.

Corresponding author: Paula Casati

Centro de Estudios Fotosintéticos y Bioquímicos (CEFOBI), Universidad Nacional de Rosario, Suipacha 531, 2000 Rosario, Argentina. TE/FAX: 0054-341-4371955

E-mail: casati@cefobi-conicet.gov.ar

ABSTRACT

ASF1 is a key histone H3/H4 chaperone that participates in a variety of DNA and chromatin-related processes, including DNA repair, where chromatin assembly and disassembly is of primary relevance. Information concerning the role of ASF1 proteins in post-UV response in higher plants is currently limited. In *Arabidopsis thaliana*, an initial analysis of *in vivo* localization of ASF1A and ASF1B indicates that both proteins are mainly expressed in proliferative tissues. *In silico* promoter analysis identified *ASF1A* and *ASF1B* as potential targets of E2F transcription factors. These observations were experimentally validated, both *in vitro* by electrophoretic mobility shift assays, and *in vivo* by chromatin immunoprecipitation assays and expression analysis using transgenic plants with altered levels of different E2F transcription factors. These data suggest that ASF1A and ASF1B are regulated during cell cycle progression through E2F transcription factors. In addition, we found that ASF1A and ASF1B are associated with the UV-B induced DNA damage response in *A. thaliana*. Transcript levels of *ASF1A* and *ASF1B* were increased following a UV-B-treatment. Consistent with a potential role in ultraviolet-B (UV-B) response, RNAi silenced plants of both genes showed increased sensitivity to UV-B compared to wild type plants. Finally, by coimmunoprecipitation analysis, we found that ASF1 physically interacts with N-terminal acetylated histones H3 and H4, and with acetyltransferases of the HAM subfamily, which are known to be involved in cell cycle control and DNA repair, among other functions. Together, here we provide evidence that *ASF1A* and *ASF1B* are regulated by cell cycle progression and are involved in DNA repair after UV-B irradiation.

INTRODUCTION

Plants, because of their sessile condition and their requirement of sunlight for photosynthesis, are inevitably exposed to ultraviolet-B radiation (UV-B, 290-315 nm), which causes direct damage to DNA, proteins, lipids, and RNA (Britt, 1996; Jansen et al., 1998; Gerhard et al., 1999; Casati and Walbot, 2004a). Thus, plants have not only developed mechanisms that filter or absorb UV-B to protect them against DNA damage (Bieza and Lois, 2001; Mazza et al., 2000), but also have different DNA repair systems to remove or tolerate DNA lesions (Bray and West, 2005; Hays, 2002; Kimura and Sakaguchi, 2006).

Absorption of UV-B by DNA induces the formation of cyclobutane pyrimidine dimers (CPD) and, to a lesser extent, pyrimidine (6-4) pyrimidone photoproducts (6-4PPs) (Friedberg et al., 1995). These lesions disrupt base pairing and block DNA replication and transcription if photoproducts persist, or result in mutations if photoproducts are bypassed by error-prone DNA polymerases (Britt, 1996). Therefore, accumulation of such lesions must be prevented to maintain genome integrity, plant growth and seed viability. At the genome level, the accessibility of DNA sequences is determined by the structure of chromatin, which is subjected to epigenetic regulation. The structure of the chromatin can be remodeled in several ways, including nucleosome assembly/disassembly: replacement of canonical histones with histone variants, covalent modifications of histones, such as phosphorylation, acetylation, methylation, ubiquitylation, sumoylation; ATP-dependent reorganization and positioning of DNA-histones; and DNA methylation (Verbsky and Richards, 2001; Pfluger and Wagner, 2007; Eberharter and Becker, 2002; Vaillant and Paszkowski, 2007).

The efficient spontaneous assembly of nucleosomes is precluded by the strong electrostatic interactions between DNA and histones. Consequently, proteins known as histone chaperones facilitate the assembly and disassembly of nucleosomes by interacting with the corresponding histones (Park et al., 2008; Avvakumov et al., 2011). Histone chaperones are conserved in eukaryotes and are classified as either H3–H4 or H2A–H2B types, according to their activity. In *Arabidopsis thaliana*, the best studied are the H3–H4 chaperones: CHROMATIN ASSEMBLY FACTOR-1 (CAF-1), HISTONE REGULATORY HOMOLOG A (HIRA) and ANTI-SILENCING FUNCTION1 (ASF1) and the H2A–H2B chaperones: NUCLEOSOME ASSEMBLY PROTEIN1 (NAP1), NAP1-RELATED PROTEINS (NRPs), and FACILITATES CHROMATIN TRANSCRIPTION (FACT) (Zhu et al., 2012).

ASF1 was originally identified by its ability to derepress transcriptional silencing when over-expressed in *Saccharomyces cerevisiae* (Le et al., 1997; Singer et al., 1998). In yeast and animals, ASF1 proteins play important roles in chromatin-related processes, such as transcription, DNA replication and repair. They participate both in the replication-dependent and the replication-independent chromatin assembly pathways, as ASF1 co-purifies with the replication-specific histone H3.1; and with the transcription-specific HISTONE H3.3 and HIRA, respectively (Myung et al., 2003;

Prado et al., 2004; Ramey et al., 2004; Franco et al., 2005; Adkins et al., 2004; Tyler et al., 1999; Tagami et al., 2004; Zhang et al., 2005; Tang et al., 2006). In *A. thaliana*, there are two genes encoding ASF1 homologues, *AtASF1A* and *AtASF1B* (At1g66740 and At5g38110, respectively; Zhu et al., 2011). Both proteins bind histone H3, and are localized in the cytoplasm and the nucleus. Mutants in either *AtASF1A* or *AtASF1B* show no obvious defects, while the double mutant shows inhibition of plant growth and abnormal vegetative and reproductive organ development. In addition, *Atasf1ab* plants exhibit cell number reduction, S-phase delay and reduced endopolyploidy levels (Zhu et al., 2011). Double mutants also show selective increased expression of *CYCB1;1* (gene involved at the G2 to M transition), genes required for S-phase checkpoint and for DNA damage checkpoint and repair, suggesting that these histone chaperones are implicated in cell cycle regulation. However, reports on *A. thaliana* ASF1 are still limited. Even more, there is no information on the role of ASF1 in post-UV response in higher plants. In this work, we have addressed the cell cycle regulation of ASF1 expression and its potential role in post-UV-B response in relation to its known function as a histone chaperone. First, we analyzed the *in vivo* localization of ASF1A and ASF1B, showing that both proteins are mainly expressed in proliferative tissues. We then analyzed their regulation by E2F transcription factors and experimentally validated *ASF1A* and *ASF1B* as targets of these transcription factors, which have a pivotal role in controlling cell-cycle progression. In addition, using transgenic plants with decreased transcript levels of both *ASF1A* and *ASF1B*, we demonstrate that ASF1A and ASF1B contribute to the UV-B induced DNA damage response in *A. thaliana*. In fact, *ASF1A* and *ASF1B* transcripts increased following a UV-B-treatment; and *asf1a/asf1b* RNAi transgenic seedlings accumulated more DNA damage after UV-B exposure compared to wild-type (WT) plants. Finally, by coimmunoprecipitation analysis, we found that ASF1 interacts with N-terminal acetylated H3 and HAM1/HAM2 histone acetyltransferases. HAM1/HAM2 are related to human TIP60, which is involved in cell cycle control, regulation of apoptosis, DNA repair as well as acting as a coactivator for a wide range of transcription factors (Sapountzi et al., 2006). Together, our data provide evidence that both *ASF1A* and *ASF1B* are regulated during cell cycle progression and participate in UV-B induced DNA damage repair.

RESULTS

ASF1A and *ASF1B* are Expressed in Actively Dividing Cells

It was previously demonstrated, by RT-PCR analysis, that both *AtASF1A* and *AtASF1B* genes were ubiquitously expressed in most of the *Arabidopsis* plant tissues analyzed (Zhu et al., 2011). To study the spatio-temporal expression of *ASF1A* and *ASF1B* in more detail, we constructed transgenic plants expressing the ß-glucuronidase (*GUS*) gene under the *ASF1A* (*ASF1A-GUS*) and *ASF1B* (*ASF1B-GUS*) promoters as described in Materials and Methods. At least four independent transgenic lines with comparable GUS activity levels were analyzed.

Expression of *ASF1A* is high in cotyledons and in the shoot apical region (Fig. 1A). *ASF1A* is also expressed in the roots of 10-d-old plants (Fig 1B). In 10-d-old seedlings, *ASF1A* is restricted to the shoot apical meristem, roots and proliferating leaves (Fig. 1C-D), while in mature leaves, *ASF1A* expression is restricted to the hydatodes at the leaf margin (Fig. 1E). In flowers, *ASF1A* expression is mainly detected in developing anthers and pistils (Fig. 1G). Siliques also show GUS activity, mainly in the dehiscence region (Fig. 1F). Reporter activity of *ASF1B-GUS* is similar but weaker than that of *ASF1A-GUS* (Fig. 1H-Q). Taken together, our results indicate that both *ASF1A* and *ASF1B* are expressed in highly dividing tissues, and their expression seems to be redundant, at least, in unstressed conditions, consistent with the phenotype of single *asf1* mutants (Zhu et al., 2011).

ASF1A and *ASF1B* are Regulated by E2F Transcription Factors

The E2F transcription factors are key components of the cyclin/retinoblastoma/E2F pathway that control cell cycle transitions in multicellular organisms (Gutierrez et al., 2002). In humans, ASF1B is regulated by E2F transcription factors during cell cycle progression (Hayashi et al., 2007). Moreover, in plants, Vandepoele et al. (2005) were able to identify that *ASF1A* and *ASF1B* are among the 181 putative E2Fa-DPa target genes. To validate these observations, we investigated the regulation of *ASF1A* and *ASF1B* genes by the E2F family.

Arabidopsis contains six functional *E2F* genes, which according to their structural and functional characteristics can be divided into two different groups. The first group includes AtE2Fa (At2g36010), AtE2Fb (At5g22220) and AtE2Fc (At1g47870) that possess a conserved DNA binding site, a heterodimerization domain and a transactivation domain embracing a retinoblastoma-related (RBR) binding site. These E2F factors associate with a DP protein (AtDPa or AtDPb) to form a functional heterodimer which can specifically recognize E2F *cis*-elements, transactivate E2F-responsive reporter genes and be negatively regulated by RBR protein (Shen, 2002; Mariconti et al., 2002). The second group includes AtE2Fd/DEL2 (At5g14960), AtE2Fe/DEL1 (At3g48160) and

AtE2Ff/DEL3 (At3g01330), which contain two conserved DNA binding domains and lack a dimerization domain (Shen, 2002; Mariconti et al., 2002).

We first searched for putative E2F binding sites 1 kb upstream of the start codon of *ASF1A* and *ASF1B* genes (Fig. 2A). Our analysis revealed the presence of one consensus E2F binding site for *ASF1A* gene: TAACCGCCC (at -330 bp from the putative ATG) in reverse orientation, and two consensus E2F binding sites for the *ASF1B* gene: TCTCCCGCCAAT (at -276 bp), containing a double palindromic sequence, and TCTCGCGCC (at -138 bp). These data are consistent with previous reports which identified *ASF1A* and *ASF1B* as putative targets of E2Fa-DPa (Vandepoele et al., 2005; Naouar et al., 2009).

To experimentally validate whether the bioinformatically identified E2F sites in the *ASF1A* and *ASF1B* promoters mediate E2F binding, we carried out electrophoretic mobility shift assay (EMSA) using labeled double-stranded oligonucleotides either corresponding to each of the E2F sites found in the *ASF1A* (Supplemental Table SI, Fig. 2B) and *ASF1B* promoters (Supplemental Table SI, Fig. 2C and D). Recombinant Arabidopsis E2Fa-DPa, E2Fe/DEL1 and E2Ff/DEL3 proteins bound to all these probes in a specific and E2F site-dependent manner (Fig. 2B-D). Thus, addition of a competitor oligonucleotide containing a general E2F consensus site (TTTCGCGC, SupplementalTable SI, Fig. 2B-D) eliminated the specific complex, but the yield of preformed complexes was unaffected when the reaction was performed with a mutated version of the consensus sequence (TTTCGATC, Supplemental Table SI, Fig. 2B-D). Therefore, E2Fs members of the two groups are able to bind *in vitro* to each of the three sites analyzed, suggesting that these transcription factors could regulate the *in vivo* expression of both genes.

To test this hypothesis, we used a set of transgenic Arabidopsis seedlings with altered E2F expression (Ramirez-Parra and Gutierrez, 2007) and analyzed *ASF1A* and *ASF1B* mRNA levels in these plants by quantitative RT-PCR (RT-qPCR, Supplemental Table SII). *CELL DIVISION CYCLE 6a* (*CDC6a,* At2g29680), a well-characterized E2F target gene (Castellano et al., 2001), was used as a positive control. Figure 3A shows an increase in both *ASF1A* and *ASF1B* transcript levels in plants which overexpress the E2Fa, E2Fb and E2Ff/DEL3. Overexpression of the transcriptional repressor E2Fc contributed to repress the expression of both *ASF1A* and *ASF1B* genes. Moreover, mRNA levels for *ASF1B* are also increased in plants that overexpress the atypical E2Fs: E2Fd/DEL2 and E2Fe/DEL1 (Fig. 3A). It is interesting to note that induction of *ASF1B* levels were always higher than those of *ASF1A* in all the transgenic plants analyzed (Fig. 3A).

Finally, *ASF1A* and *ASF1B* transcript levels were analyzed in plants overexpressing RepA, a viral protein which increases endogenous E2F activity by inactivating the RBR protein through physical interaction, and in plants overexpressing a mutated version of RepA protein (RepA E198K), in which RBR interaction is abolished (Desvoyes et al., 2006). Figure 3B shows that *ASF1B* mRNA levels are higher in the RepA expressing plants relative to the RepA mutant plants, while *ASF1A* levels are similar in both plants.

In addition, chromatin immunoprecipitation (ChIP) experiments were performed using commercial antibodies that recognize haemaglutinin (HA) or anti-myc antibodies with transgenic Arabidopsis plants that overexpress HA-E2Fe (*E2Fe*^{OE}), HA-E2Ff (*E2Ff*^{OE}) (Ramirez-Parra et al., 2004) or myc-E2Fd (*E2Fd*^{OE}; Ramirez-Parra and Gutierrez, 2007) fusion proteins. We chose to use these plants because (i) they show high induction (see Fig. 3A), (ii) these E2F do not need a DP and (iii) they do not interact with RBR, which may simplify the interpretation of data (Mariconti et al., 2002; Lammens et al., 2008). Arabidopsis WT plants were used as a negative control. Genomic immunoprecipitated DNA was screened by PCR for the presence of promoter regions of *ASF1A* and *ASF1B*. Primers for the promoter region of *ACTIN2* (*ACT2,* At3g18780), a non E2F-regulated gene, were used as a negative control, while primers designed to amplify a promoter region of the *MCM3* gene (At5g46280), which is regulated by E2F factors (Stevens et al., 2002), were used as a positive control (Supplemental Table SIII). After 34 PCR cycles, total input DNA from sonicated nuclei generated positive amplification signals with all the primers used (Fig. 3C). Likewise, promoter fragments of *ASF1A* and *ASF1B,* and the positive control *MCM3* that contains E2F binding sites were significantly amplified from the anti-HA immunoprecipitates of *E2Ff*^{OE} and *E2Fe*^{OE} plant extracts, and from the anti-myc immunoprecipitates of *E2Fd*^{OE} extract (Fig. 3C). However, no or very low amplification was obtained either when primers specific for the promoter of *ACT2* were used (Fig. 3C). Taken together, these results demonstrate that E2F family members can bind to both *ASF1A* and *ASF1B* promoters *in vitro* and *in vivo*, and regulate the expression of both genes.

To further validate the cell cycle regulation of *ASF1A* and *ASF1B*, their expression was investigated in microarray data generated using the Genevestigator© tool package. Data was obtained from experiments done using Arabidopsis cultured cells synchronized by sucrose starvation for 24 h (Hennig et al, 2003). Samples were collected at the indicated times after release from the sucrose block (Supplemental Fig. S1). *ASF1A,* and in particular, *ASF1B* transcript levels were compared at each time, together with *MCM3* and *CYCB1.4* (At2g26760) as markers for up-regulated genes at the G1/S and G2/M transition, respectively and with *ACT2* that remains constant during the cell cycle. These results demonstrate that both *ASF1A* and *ASF1B* are regulated during the cell cycle and show higher expression during S phase (Supplemental Fig. S1). These results are consistent with these genes being targets of E2F transcription factors.

Transgenic Plants with Decreased *ASF1A* and *ASF1B* mRNA Levels Show Decreased Rosette Area Compared to that of WT Plants

To gain insight into *AtASF1A* and *AtASF1B* function, seeds of RNAi plants with decreased levels of both *ASF1A* and *ASF1B* (lines CS3995, CS3996 and CS30921) were obtained from the Plant Chromatin Consortium (http://www.chromdb.org). By RT-qPCR, we found that expression of *ASF1A* is decreased about three-fold in three independent transgenic lines (Fig. 4A), while *ASF1B* is

decreased about ten-fold (Fig. 4B). It is interesting to note that the RNAi construction was made to target *ASF1B*; however, as the sequences of both genes are highly similar (Zhu et al., 2011), the RNAi construct is able to silence both genes, at least partially. Figures 4C and 4D show that RNAi transgenic plants show decreased rosette area compared to that of WT plants, indicating probable defects in cell proliferation or cell expansion. Interestingly, Zhu et al. (2011) previously reported that loss of function of either *AtASF1A* or *AtASF1B* did not show obvious defects, but the average surface area of leaf blade of the double mutant *Atasf1ab* was about 60% of that of WT because of a reduction in the numbers of palisade and pavement cells, S-phase delay/arrest, and reduced polyploidy levels, suggesting that ASF1 proteins are involved in the control of the cell cycle progress.

ASF1 interacts with Acetylated H3 and H4 Histones, and with HAM1/HAM2 Histone Acetylase

Histone acetylation is mediated by histone acetyltransferases (HATs)/deacetylases (HDACs). In Arabidopsis, there are four different families of HATs and three families of HDACs (Pandey et al., 2002). The HATs families (http://www.chromdb.org) include: the p300/CREB binding protein (CBP) family (HAC, 5 genes), the GCN5-related N-terminal acetyltransferases (GNAT) superfamily (HAG, 3 genes), the TAFII250 family (TATA binding protein-associated factors, HAF, 2 genes), and the MYST family (HAM, 2 genes). Each of these enzymes can acetylate different aminoacids residues of the histones, giving them specificity. In humans, the best characterized member of the MYST family is TIP60 (from Tat-Interacting Protein 60 kDa). TIP60 has important roles during DNA repair, gene transactivation in response to DNA damage, and more importantly, histone H4 acetylation when DNA is damaged (Squatrito et al., 2006). In addition, TIP60 not only acetylates histones, but also non-histone proteins, such as the ATM kinase, a key regulator of the DNA double-strand break (DSB) repair pathway and checkpoint activation (Sun et al., 2010).

A physical interaction in yeast between Asf1 and SAS2, a member of the MYST (MOZ, Ybf2/Sas3, Sas2, and TIP60) subfamily of acetyltransferase (Osada et al., 2001), has been previously reported. To further investigate these observations in plants, we carried out coimmunoprecipitation experiments using commercial antibodies against human ASF1A+B proteins (ABCAM ab53608). These antibodies recognized a unique band when Western blots were performed with *E. coli* crude protein extracts expressing the recombinant GST-ASF1A fusion protein (Fig. 5A). Figure 5B shows that ASF1 proteins coimmunoprecipitated with N-terminal acetylated forms of H3 and H4 histones. These results validate the proposed function of AtASF1 as histone binding protein.

Next, we analyzed the interaction of ASF1 proteins with Arabidopsis TIP60 homologues, HAM1 and HAM2. Figure 5B shows that ASF1 binds *in vivo* to a protein with the predicted molecular mass of HAM1/HAM2. This interaction was also observed when coimmunoprecipitation was carried out using antibodies against human TIP60 protein (ABCAM ab23886), and immunoblotting was

revealed using the anti-ASF1 antibodies (Fig. 5C). Thus, these results confirm the physical interaction between ASF1 and N- terminal acetylated Histones H3 and H4 and HAM in plants.

ASF1A and *ASF1B* Expression is Induced by UV-B Radiation through E2F Transcription Factors, and Both Proteins Participate in UV-B Induced DNA Damage Repair

In plants, E2F factors contribute to the transcriptional induction of genes upon DNA damage (Lincker et al., 2008; Shen, 2002; Mariconti et al., 2002; Ramirez-Parra et al., 2007). In addition, chromatin remodeling deficient plants show increased DNA damage by UV-B (Campi et al., 2012). Thus, it is possible that AtASF1 proteins may have a role during DNA damage and repair. To investigate if this is the case, we focused on the potential role of AtASF1 proteins in the UV-B induced DNA damage response pathway in plants. We first analyzed their expression after UV-B by RT-qPCR analysis in plants exposed under UV-B lamps for 4 h (2 $W.m^{-2}$) in growth chamber conditions. After the treatment, rosettes from plants of 11, 16, 19 and 28 DAS were collected for RNA extraction. Figure 6A and 6B shows that *ASF1A* and *ASF1B* transcript levels significantly increased after UV-B irradiation. Moreover, transgenic plants expressing *GUS* under the *ASF1A* and *ASF1B* promoters also show differences in the intensity of GUS histochemical staining after the UV-B treatment (Supplemental Fig. 2).

To further analyze the presence of acetylated histones H3 and H4 in *ASF1A* and *ASF1B* promoters after irradiation with UV-B, we carried out ChIP assays. Previously, we demonstrated that acetylated histones, typical marks of transcriptional active chromatin, contribute to the transcriptional response to UV-B (Casati et al., 2008, Qüesta et al., 2010). In maize lines, UV-B–tolerant lines exhibit greater acetylation on N-terminal tails of histones H3 and H4 after irradiation; and these acetylated histones are enriched in the promoter and transcribed regions of UV-B–upregulated genes. Thus, ChIP analysis was performed using commercially available antibodies specific for acetylated Lys residues in the N-terminal tails of histones H3 and H4. DNA recovered after immunoprecipitation was screened via qPCR for the presence of promoter regions of *ASF1A* and *ASF1B* (-533 to +71, and -532 to +80 from the ATG translation start sites, respectively). RT-qPCR was also performed with samples incubated in the absence of antibody to evaluate non-specific binding. All ChIP samples were normalized to total input DNA from sonicated nuclei for determining the selective recovery of gene segments. Figure 6C shows that promoter regions of both *ASF1A* and *ASF1B* were enriched significantly in the fractions immunoprecipitated with anti-acetylated H3 and anti-acetylated H4 from UV-B–irradiated samples Therefore, the increase in H3 and H4 acetylation at the promoter region correlates with the increase in *ASF1A* and *ASF1B* transcript abundance.

In parallel, regulation of different E2F factors by UV-B radiation was analyzed to determine if UV-B induction of *ASF1A* and *ASF1B* could be mediated, at least in part, by one or more of these transcription factors. For these experiments, 12 days after sown (DAS) WT Arabidopsis seedlings

were irradiated with UV-B during 4h, and mRNA levels of *E2F* factors, were assayed under control conditions and after the different UV-B treatments. Figure 6D shows that *E2Fa*, *E2Fb, E2Fc* and *E2Fd* are induced after 4h of UV-B. However, *E2Fe* and *E2Ff* are not regulated by this radiation. Therefore, UV-B regulation of *ASF1A* and *ASF1B* may be mediated by some or all the UV-B regulated E2F transcription factors.

To investigate the hypothesis that ASF1 proteins participate in DNA damage repair by UV-B radiation, we grew Arabidopsis WT and RNAi transgenic plants in the growth chamber in the absence of UV-B for 12 DAS. Plants were then exposed 4 h to UV-B radiation (2 $W.m^{-2}$), both under light conditions that allow photoreactivation (light), or in the absence of white light to analyze dark repair (dark). As a control, different plants were irradiated with the same lamps covered with a polyester plastic that absorbs UV-B (see Materials and Methods). Leaf samples from control and treated plants mantained under light and dark conditions were collected immediately or 2h after the end of the UV-B treatment, DNA was extracted and the cyclobutane pirimidine dimer (CPD) accumulation was compared in the RNAi plants relative to that in WT plants using monoclonal antibodies specifically raised against them. Comparison of the CPD accumulation in samples from WT and RNAi plants after the different UV-B treatments and in control conditions in the absence of UV-B as described in Materials and Methods are shown in Figure 6E. In the absence of UV-B, the steady state levels of CPDs in WT and RNAi plants were similar. However, after 4 h of exposure to UV-B radiation, more unrepaired lesions accumulated in the RNAi than in WT plants when plants were irradiated with UV-B in the presence of white light (Fig. 6E). This difference was not observed when plants were kept under dark conditions. Same results were obtained after 2h of recovery in the absence of UV-B. Although photoreactivation is evident in both WT and the RNAi plants after 2 h of recovery in the light, the RNAi plants still show more CPDs than WT plants (Fig. 6E). On the other hand, CPD accumulation under dark conditions was similar in both plants. Therefore, this result demonstrates that the photorepair of UV-B induced DNA lesions is less efficient in plants that are deficient in the expression of both *ASF1A* and *ASF1B*, while dark repair is not affected in the RNAi plants.

To discard the possibility that decreased expression of *ASF1A* and *ASF1B* genes may be affecting the expression of DNA-repair enzymes of other repair systems, *UVR2* (encoding a CPD photolyase; At1g12370), *UVR3* (encoding a 6-4 photoproduct photolyase; At3g15620) and *UVR7* (encoding ERCC1, a DNA excision repair protein of the nucleotide excision repair system; At3g05210) transcript levels were analyzed by RT-qPCR in WT and RNAi plants. Similar levels of both transcripts were measured in wild-type and transgenic plants, both under control conditions and after the 4h UV-B treatment (Fig. 6F). These results indicate that major CPD removal mechanisms are unaffected in mutant plants. Collectively, these results suggest that ASF1 activities participate in CPD photorepair in Arabidopsis because in the RNAi plants, chromatin is more accessible to damage accumulation, and not because ASF1 proteins regulate the expression of repair enzymes.

DISCUSSION

The deposition of histones H3/H4 onto DNA to give the tetrasome, and the removal of H3/H4 from DNA are the first and the last steps in nucleosome assembly and disassembly, respectively. ASF1 has been shown to be a H3/H4 chaperone that functions in both of these processes in yeast and other eukaryotes (Yuan and Zhu, 2012). In yeast, it was demonstrated that Asf1 shields H3/H4 from unfavorable DNA interactions, and aids the formation of favorable histone–DNA interactions through the formation of disomes (Donham et al., 2011). In addition, yeast cells lacking Asf1 display increased frequency of genome instability and spontaneous genome rearrangement (Myung et al., 2003; Prado et al., 2004; Ramey et al., 2004). ASF1 is also required to efficiently complete DNA replication in the presence of DNA damaging agents or compromised replication machinery (Franco et al., 2005). In *Drosophila melanogaster,* ASF1 was shown to assemble chromatin onto newly replicated DNA *in vitro* in synergy with CAF-1 (Tyler et al., 1999) and to co-localize with active replication forks (Schulz and Tyler, 2006). Even though information on *A. thaliana* ASF1 is limited, the results obtained so far suggest that this histone chaperone is implicated in cell cycle regulation. In this species, loss-of-function of the two Arabidopsis *ASF1* genes, *AtASF1A* and *AtASF1B*, caused S-phase delay/arrest and increased level of DNA damage (Zhu et al., 2011). Even more, it was demonstrated that ASF1B is target of TOUSLED cell-cycle-related kinase (Ehsan et al., 2004). In this work, we provide new evidence that expression of ASF1 proteins is coordinated with cell cycle progression and participate in UV-induced DNA damage repair in *A. thaliana* plants. Here, we first constructed transgenic plants expressing the GUS reporter gene directed by *ASF1A* and *ASF1B* basal promoters. Results show that both ASF1A and ASF1B proteins are mainly localized in proliferative tissues (Fig. 1), and that their expression is redundant, thus suggesting that both proteins have a role during cell proliferation.

We then investigated the regulation of *ASF1* genes by E2F transcription factors, which are key components of the RBR/E2F pathway that controls cell cycle transitions in multicellular organisms, including plants (Gutierrez et al., 2002). Our experiments show that *ASF1A* and *ASF1B* are targets of these transcription factors, both *in vitro* and *in vivo*. First, we demonstrated by both EMSA and ChIP analysis, that E2F factors bind to *ASF1A* and *ASF1B* promoters; second, transgenic plants that overexpress different E2F factors show altered levels of both *ASF1A* and *ASF1B* transcripts. Both *ASF1A* and *ASF1B* have been previously identified as putative targets of the E2F transcription factors (Vandepoele et al., 2005). The *ASF1A* promoter has one E2F-binding sequence in its basal promoter, while *ASF1B* has two E2F binding sites (Fig. 2A). All these three sites were shown to be bound *in vitro* by E2Fa-DPa, E2Fe/DEL1 and E2Ff/DEL3 (Fig. 2B-C). On the contrary, both *ASF1A* and *ASF1B* show decreased expression in plants overexpressing E2Fc, similarly as the E2F-regulated gene *CDC6a* (Fig. 3A). Arabidopsis *E2Fa* transcripts peak shortly before the S-phase, while *E2Fb* mRNAs

are higher at the G1/S transition. Both *E2Fc* and *E2Fd* increase during the progression into S-phase and show a maximum expression after the passage into G2, while *E2Fe* and *E2Ff* are expressed at the G1/S and S/G2 transitions (Mariconti et al., 2002). Therefore, our results suggest that E2F transcription factors regulate the expression of *ASF1A* and *ASF1B* genes through the cell cycle progression.

We have confirmed that ASF1 interacts with histone H3, as previously reported (Fig. 4, Zhu et al., 2011). In addition, we here demonstrate that ASF1 proteins bind to the acetylated form of this histone, and also with the N-terminal acetylated histone H4. In yeast, it was reported that Asf1 is required for the acetylation of Lysine 9 (K9) and Lysine 56 (K56) and newly synthesized H3 K56 modification is predicted to contribute to chromatin assembly (Masumoto et al., 2005; Xu et al., 2005). In addition, Adkins et al. (2007) previously proposed that Asf1 presents the newly synthesized H3 K56 for acetylation by the histone acetyltransferase Gcn5 prior to chromatin assembly.

On the other hand, in this species, Asf1 functions with a Clr6 histone deacetylase complex to silence heterochromatic repeats by promoting histone deacetylation (Yamane et al., 2011). Therefore, yeast Asf1 has a role both in histone acetylation and deacetylation. Thus, it is possible that this role may also be conserved in plants. We also found that ASF1 binds to Arabidopsis HAM1/HAM2 acetyltransferases *in vivo* (Fig. 5). In yeast, it was also demonstrated that Asf1 interacts with a SAS complex, which is a member of the MYST acetyltransferase family (Osada et al., 2001). In this species, the SAS complex promotes silencing at telomeres, providing evidence for an important role of the acetyltransferase activity of the SAS complex in silencing. Even more, yeast *asf1* mutants show silencing defects similar to mutants in the SAS complex (Osada et al., 2001). Thus, Asf1-dependent chromatin assembly may mediate the silencing role of the SAS complex. On the other hand, TIP60 interacts in various eukaryotes with multiple protein partners besides histones and promote their acetylation. In this way, TIP60 is a highly connecting protein, controlling the acetylation of a wide range of cellular proteins which are required to maintain cell viability (for a review, see Sun et al., 2010). One substrate of TIP60 is the ATM protein kinase, which is a key regulator of DSB repair pathway. Following DSB production, inactive ATM-Tip60 complex is recruited to the DSB by the mre11-rad50-nbs1 (MRN) complex. Tip60 chromodomain then interacts with histone H3 trimethylated on lysine 9, activating Tip60 acetyltransferase activity and stimulating the subsequent acetylation and activation of ATM kinase activity. Active ATM kinase phosphorylates proteins involved in both checkpoint activation and DNA repair. Thus, chromatin structure regulates DNA damage signaling and histone modifications co-ordinate DNA repair (Sun et al., 2010). In accordance to these data, plant *ham1* and *ham2* mutants show increased DNA damage after UV-B irradiation (Campi et al., 2012). Therefore, the interaction between ASF1 and HAM proteins may be crucial to regulate cell cycle progression after a genotoxic stress.

Both *ASF1A* and *ASF1B* transcripts are increased following a UV-B-treatment; and this UV-B regulation may be, at least in part, mediated by some E2F factors, as *E2Fa*, *E2Fb*, *E2Fc* and *E2Fd*

mRNAs are rapidly increased by our UV-B treatment (Fig. 6D) In this respect, transgenic plants with decreased transcript levels of both *ASF1A* and *ASF1B*, accumulate more DNA damage after UV-B exposure compared to WT plants at the seedling stage (Fig. 6D). Our results also demonstrate that the photorepair of UV-B induced DNA lesions is less efficient in plants that are deficient in the expression of both *ASF1A* and *ASF1B*, while dark repair is not affected in the RNAi plants. Moreover, we here demonstrate that major CPD removal mechanisms are unaffected in mutant plants; suggesting that ASF1 activities participate in CPD photorepair in Arabidopsis because in the RNAi plants, chromatin is more accessible to damage accumulation, and not because ASF1 proteins regulate the expression of repair enzymes. In yeast, Asf1 and the checkpoint kinase Rad53 are found in a complex in budding yeast cells in the absence of genotoxic stress (Jiao et al., 2012). Upon replication stress caused by hydroxyurea, the Asf1-Rad53 complex dissociates suggesting that the complex is regulated by genotoxic stress conditions (Jiao et al., 2012). In addition, Asf1 is important for transcriptional derepression of two DNA damage response (DDR) genes during the S phase in response to hydroxyurea (Minard et al., 2011). The contribution of Asf1 to DDR gene derepression depends on its ability to stimulate H3K56 acetylation by lysine acetyltransferase Rtt109 (Minard et al., 2011). In addition, as mentioned earlier, in Arabidopsis, ASF1B is phosphorylated by the TOUSLED protein kinase (TLS) (Ehasan et al., 2004). Arabidopsis *tls* mutants are highly sensitive to genotoxic stress, including UV-B radiation (Wang et al., 2007). Even more, in humans, Sen et al. (2006) provided evidence that TLK1B protects against UV radiation, via Asf1-mediated chromatin assembly at the sites of UV damage. Therefore, participation of ASF1 proteins in DNA damage responses seems to be a mechanism to prevent cell cycle progression when damaged DNA accumulates, and this participation is probably regulated by the action of UV-B regulated E2F transcription factors. In this way, organisms may adapt to environmentally harsh conditions by cell cycle reprogramming to ensure optimal growth.

In conclusion, in this work we provide new evidence of the regulation of *AtASF1A* and *AtASF1B* by E2F factors and DNA damage. Our analysis showed that *ASF1A* and *ASF1B* are targets of the E2F transcription factors. In addition, we demonstrated that both *ASF1A* and *ASF1B* transcripts are present in proliferative tissues and are increased by UV-B irradiation in this species. We also observed that UV-B induced the accumulation of CPDs in *asf1a/asf1b* RNAi transgenic plants relative to WT plants. Finally, we found physical interaction between ASF1, and N-terminal acetylated Histones H3 and H4 and HAM acetyltransferases, proteins known to be involved in cell cycle control and DNA repair, among other functions. Together, our data provide evidence that both ASF1A and ASF1B proteins are regulated during cell cycle progression and participate in UV-induced DNA damage response.

MATERIALS AND METHODS

Plant Material and Growth Conditions

Arabidopsis (*A. thaliana* Col-0 ecotype) seeds were sown on soil and placed at 4ºC in the dark. After 3 days, pots were transferred to a greenhouse and plants were grown at 22ºC under a 16h/8h light/dark regime. For *in vitro* growth of plants, seeds were sterilized and incubated at 4ºC for 72 h before plating on MS (Murashige and Skoog salt) medium supplemented with 1.5 % (w/v) sucrose and 0.8 % (w/v) agar.

RNAi lines (CS3995, CS3996 and CS30921) were obtained from the Arabidopsis Biological Resource Center (ABRC, Columbus, OH). These lines confer silencing to the *ASF1B* target gene. Specific reduction of target mRNA was measured by RT-qPCR. *A. thaliana* ecotype Wassilewskija (Ws) was the background used for assays using RNAi lines. We also used plants expressing the geminivirus RepA, either wild-type or E198K point mutant that abolishes interaction with RBR (Desvoyes et al., 2006), and plants with altered levels of different E2Fs (Ramirez-Parra et al., 2007).

For expression analysis, a 780 bp region containing the *AtASF1B* promoter or a 655 bp region containing the *AtASF1A* promoter were amplified by PCR (using primers shown in Supplemental Table SIV) and fused to the *GUS* coding sequence in pBI101.1 vectors (Jefferson et al., 1987). These fusion constructs (*pAT-ASF1A:GUS* and *pAT-ASF1B:GUS*) were transformed in Arabidopsis (Col-0 ecotype) plants using *Agrobacterium tumefaciens* C58CRifR by the floral dip method (Clough and Bent, 1998). Transformed seedlings (T0 generation) were selected on MS agar plates containing 50 mg ml^{-1} of kanamycin and transferred to soil. T2 homozygous plants were selected for further analysis. Histochemical detection of GUS activity was carried out using 5-bromo-4-chloro-3-indolyl-β-D-glucuronide (Jefferson et al., 1987).

Electrophoretic Mobility Shift Assays

DNA binding assays were performed as described previously (Ramirez-Parra and Gutierrez, 2000). Briefly, reactions (20 µl) contained 20 mM HEPES, pH 7.9, 12 % (v/v) glycerol, 50 mM KCl, 1 mM DTT, 1 mM EDTA, 1 mM $MgCl_2$, double-stranded oligonucleotides containing E2F sites as probes (Supplemental Table SI), 1 µg of salmon sperm DNA as nonspecific competitor and 200 ng of E2F proteins, as indicated. Proteins were obtained as previously described (Ramirez-Parra and Gutierrez, 2000). For competition experiments, 100-fold of annealed unlabeled probe or unlabeled mutated probe (Supplemental Table SI) was included in the reactions. After incubation at 4°C for 20 min, DNA–protein complexes were loaded onto 4% native polyacrylamide gels and electrophoresed in 0.5X TBE buffer. Labeled DNA-protein complexes were visualized by autoradiography.

RT-qPCR

Total RNA was isolated from about 100 mg of tissue using the TRIzol reagent (Invitrogen, Carlsbad, CA) as described by the Manufacturer's Protocol. The RNA was incubated with RNase-free DNase I (1 U/ml) following the protocol provided by the manufacturer to remove possible genomic DNA. Then, RNA was reverse-transcribed into first-strand cDNA using SuperScript II reverse transcriptase (Invitrogen) and oligo-dT as a primer. The resultant cDNA was used as a template for qPCR amplification in a MiniOPTICON2 apparatus (Bio-Rad), using the intercalation dye SYBRGreen I (Invitrogen) as a fluorescent reporter and Platinum Taq DNA Polymerase (Invitrogen). Primers for each of the genes under study were designed using the PRIMER3 software (Rozen and Skaletsky, 2000) in order to amplify unique 150-250 bp products (Supplemental Table SII). Amplification conditions were carried out under the following conditions: 2 min denaturation at 94°C; 40 to 45 cycles at 94°C for 15 s, 57°C for 20 s, and 72°C for 20 s, followed by 10 min extension at 72°C. Three replicates were performed for each sample. Melting curves for each PCR were determined by measuring the decrease of fluorescence with increasing temperature (from 65ºC to 98ºC). PCR products were run on a 2 % (w/v) agarose gel to confirm the size of the amplification products and to verify the presence of a unique PCR product. Gene expressions were normalized to the *A. thaliana* Actin 8 *(ACT8,* At1g49240*)* or calcium dependent protein kinase3 (*CPK3*, At4g23650). The expression of *CPK3* has been previously reported to remain unchanged by UV-B (Casati and Walbot, 2004b; Ulm et al., 2004).

UV-B Irradiation Treatments

For analysis of gene expression, DNA damage and ChIP experiments, Arabidopsis plants were exposed for 4 h to UV-B radiation from UV-B bulbs (Bio-Rad, Hercules, CA, USA) in a growth chamber. UV-B lamps were covered with cellulose acetate filters (100 µm extra clear cellulose acetate plastic; Tap Plastics, Mountain View, CA, USA) and placed 30 cm above the plants, in order to only exclude UV-C, but not remove UV-B and UV-A radiation from the spectrum. The UV intensities measured with a UV-B/UV-A radiometer (UV203 AB radiometer; Macam Photometrics, Scotland, UK) were 2 W m^{-2} and 0.65 W m^{-2} for UV-B and UV-A, respectively. Control plants (without supplemental UV-B radiation) were exposed for the same period of time to light sources described above but covered with polyester filters (100 µm clear polyester plastic; Tap Plastics). This polyester filter absorbs both UV-B (0.04 W m^{-2}) and wavelengths < 280 nm (UV-A radiation intensity was 0.4 W m^{-2}). Immediately after irradiation, samples from at least three independent biological replicates were collected, frozen in liquid nitrogen, and stored at –70 $^{\circ}$C.

DNA Damage Analysis

CPD accumulation was measured as previously described (Lario et al., 2011). For the assay, leaf samples of 12 DAS were used. Samples were collected from control and UV-B treated plants. UV-B treatments were performed both under light or dark conditions; plants irradiated under dark conditions were allowed to recover for 2h under light or dark conditions. After the different treatments, plant samples (0.1 g) were collected and immediately immersed in liquid nitrogen and stored at -70ºC. DNA was extracted by a modified cetyl-trimetyl-ammonium bromide (CTAB) method, denatured in 0.3 M NaOH for 10 min and six-fold dot blotted onto a nylon membrane (Perkin Elmer Life Sciences, Inc.). The membrane was incubated for 2 h at 80ºC and then blocked in TBS (20 mM Tris-HCl, pH 7.6, 137 mM NaCl) containing 5 % (w/v) dried milk for 1 h at room temperature. The blot was then washed with TBS and incubated with TDM-2 (1:2000 in TBS) overnight at 4ºC with agitation. Monoclonal antibodies specific to CPDs (TDM-2) were from Cosmo BioCo., Ltd. (Japan). Unbound antibody was washed away and secondary antibody (BioRad) conjugated to alkaline phosphatase (1:3000) in TBS was added. The blot was then washed several times and subsequently developed with 5-bromo-4-chloro-3-indolyl phosphate and nitro blue tetrazolium. Quantification was achieved by densitometry of the dot blot using ImageQuant software version 5.2. DNA concentration was fluorometrically determined using the Qubit dsDNA assay kit (Invitrogen), and checked in a 1 % (w/v) agarose gel stained with SYBR Safe after quantification.

Chromatin immunoprecipitation (ChIP) assays

ChIP assays and data analysis were carried out basically as previously described (Ramirez-Parra et al., 2004). Briefly, whole 12 DAS WT or E2Fd (E2Fd^{OE}), E2Fe (E2Fe^{OE}), E2Ff (E2Ff^{OE}) overexpressing plants were treated with 1% (v/v) formaldehyde under vacuum. Crosslinking reaction was then stopped with 0.125 M glycine. Nuclei were extracted, lysed in SDS buffer (50 mM Tris-HCl, pH 8, 10 mM EDTA, 1% (w/v) SDS) and sonicated to shear DNA to an average size of 700-1500 bp. Crude chromatin lysates were precleared with protein G agarose beads (Santa Cruz Biotech.), blocked with salmon sperm DNA, and then incubated overnight at 4ºC with anti-HA (Roche) or anti-myc 9E0 (Santa Cruz Biotech.) antibodies, as indicated. Immunocomplexes were recovered using protein G agarose, extensively washed and eluted from beads. Crosslinks were reversed and samples were treated with proteinase K. DNA was then extracted by phenol/chloroform method, ethanol precipitated and resuspended in 50 µl of water. Aliquots (1 µl) were used for PCR. Sequences of used primers are shown in Supplemental Table SIII. To measure the levels of acetylation of histones in the promoter regions of *ASF1A* and *ASF1B* upon UV-B treatment, the following antibodies were used: 4 µl of anti-N-terminal acetylated H4 or 4 µl of anti-N-terminal acetylated H3 (06-598 and 06-599, respectively, Upstate Biotechnology, LakePlacid, NY). The antibodies used were previously tested for crossreactivity against maize proteins (Casati et al., 2008; Qüesta et al., 2010). Three

biological replicates of chromatin immunoprecipitation (ChIP) assays were performed from each sample type, and three qPCR experiments were done with each sample.

Isolation of nuclei and coinmunoprecipitation

Nuclei were isolated from 12 DAS WT Arabidopsis seedlings essentially as described by Gallagher and Ellis (1982). Seedlings (6 g) were grinded with 25 ml of buffer 1 (0.4 M sucrose, 10 mM Tris-HCl, pH 8, 10 mM $MgCl_2$, 5 mM 2-mercaptoethanol, and 0.1 mM PMSF) in liquid N_2. The mixture was filtered through four layers of Miracloth and centrifuged at 5000*xg* for 20 min at 4ºC. The pellet was gently resuspended in 7 ml of buffer 2 (0.25 M sucrose, 10 mM Tris-HCl, pH 8, 10 mM $MgCl_2$, 5 mM 2-mercaptoethanol, 0.1 mM PMSF and 0.15% (v/v) Triton X-100) and then centrifuged at 12,000*xg* for 10 min at 4ºC. The pellet was resuspended in 4 ml of buffer 3 (0.44 M sucrose, 25 mM Tris-HCl, pH 7.6, 10 mM $MgCl_2$, 10 mM 2-mercaptoethanol, 2.5% (w/v) Ficoll F400, 5% (w/v) dextran T40, and 0.5% (v/v) Triton X-100) and layered onto a Percoll step gradient, consisting of 2 ml of 40%, 60%, and 80% (v/v) Percoll. Percoll buffer contained 0.44 M sucrose, 25 mM Tris-HCl, pH 7, and 10 mM $MgCl_2$ (Buffer 4). After centrifugation at 2500*xg* for 30 min, nuclei banded at the surface of the sucrose pad. Nuclei were then washed twice with buffer 3 and suspended in buffer 5 (0.44 M sucrose, 50 mM Tris-HCl, pH 7.0, 5 mM $MgCl_2$, 10 mM 2-mercaptoethanol, and 20% (v/v) glycerol). After centrifugation at 12000*xg* for 10 min, the pellet was resuspended in lysis buffer (10 mM Tris-HCl, pH 7.5, 1% (v/v) Triton X-100, 500 mM NaCl, 1 mM PMSF and 10% (v/v) glycerol) and sonicated. Finally, after centrifugation at 22,000*xg* for 15 min, the supernatant was frozen at -20ºC. For immunoprecipitation experiments, 250 µl of nuclear extract was combined with 1 µl anti-ASF1A+B (ABCAM ab53608) or 2 µl of anti-TIP60 (ABCAM ab23886) and rotated end-over-end at 4°C for 3 h. Protein G-agarose beads (20 µl; Boehringer Mannheim) were added and the incubation was continued for 1 h. Immuno-complexes were washed four times with 1 ml ice-cold extraction buffer (100 mM Tris-HCl, pH 7.5, 150 mM NaCl, 1% (v/v) Triton X-100 and 1 mM EDTA), resuspended in 50 µl SDS/PAGE sample buffer (50 mM Tris-HCl pH 6.8, 2% (w/v) SDS, 10% (v/v) glicerol, 2 mM β-mercaptoethanol, 12.5 mM EDTA, 0.02 % (w/v) bromophenol blue) heated to 70°C for 5 min and analyzed by SDS-PAGE followed by immunodetection according to Burnette (1981). Commercial IgG fractions were used for the detection of N-terminal acetylated H4, N-terminal acetylated H3 (06-598 and 06-599, respectively, Upstate Biotechnology, LakePlacid, NY) and histone acetyl transferase (HAM). Bound antibodies were visualized by goat anti-rabbit or anti-mouse IgG conjugated to alkaline phosphatase according to the manufacturer's instructions (Bio-Rad). The molecular masses of the polypeptides were estimated from a plot of the log of the molecular masses of marker standards (Bio-Rad) versus migration distance.

Rosette area quantification

Approximately, 20 seeds per tray were sowed leaving enough space between them to avoid superposition during plant growth. A group of 14 DAS plants were subjected to 4h UV-B treatment (2 W m^{-2}) and another group was kept as control plants; after the treatment all the plants were kept in the growth chamber under a 16h/8h light/dark regime until the end of the experiment. Every 3 days, photographs were taken and rosette area of each plant was measured.

Accession Numbers

Sequence data from this article can be found in the Arabidopsis Genome Initiative under the following locus: At1g66740 (*ASF1A*), At5g38110 (*ASF1B*) At2g36010 (*E2Fa*), At5g22220 (*E2Fb*), At1g47870 (*E2Fc*), At5g14960 (*E2Fd/DEL2*), At3g48160 (*E2Fe/DEL1*), At3g01330 (*E2Ff/DEL3*). At3g12280 (*RBR*), At2g29680 (*CDC6a*), At4g23650 (*CPK3*), At3g18780 (*ACT2*), At5g46280 (*MCM3*), At1g49240 (*ACT8*).

ACKNOWLEDGMENTS

We thank the Arabidopsis Biological Resource Center (ABRC, Columbus, OH) that provided seed stocks.

LITERATURE CITED

Adkins MW, Howar SR, Tyler JK (2004) Chromatin disassembly mediated by the histone chaperone Asf1 is essential for transcriptional activation of the yeast *PHO5* and *PHO8* genes. Mol Cell **14:** 657–666

Adkins MW, Williams SK., Linger J, Tyler JK (2007) Chromatin disassembly from the PHO5 promoter is essential for the recruitment of the general transcription machinery and coactivators. Mol Cell Biol **27:** 6372-6382

Avvakumov NA, Nourani J, Cote J (2011) Histone chaperones: modulators of chromatin marks. Mol Cell **41:** 502–514

Bieza K, Lois R (2001) An Arabidopsis mutant tolerant to lethal ultraviolet-B levels shows constitutively elevated accumulation of flavonoids and other phenolics. Plant Physiol **126:** 1105-1115.

Bray CM, West CE (2005) DNA repair mechanisms in plants: crucial sensors and effectors for the maintenance of genome integrity. New Phytol **168:** 511–528

Britt AB (1996) DNA damage and repair in plants. Annu Rev Plant Physiol Plant Mol Biol **47:** 75-100

Burnette WN (1981) "Western blotting": electrophoretic transfer of proteins from sodium dodecyl sulfate-polyacrylamide gels to unmodified nitrocellulose and radiographic detection with antibody and radioiodinated protein A. Anal Biochem **112:** 195–203

Campi M, D'Andrea L, Emiliani J, Casati P (2012) Participation of Chromatin-Remodeling Proteins in the Repair of Ultraviolet-B-Damaged DNA. Plant Physiol **158:** 981–995

Casati P, Walbot V (2004a) Crosslinking of ribosomal proteins to RNA in maize ribosomes by UV-B and its effects on translation. Plant Physiol **136:** 3319-3332

Casati P, Walbot V (2004b) Rapid transcriptome responses of maize to UV-B in irradiated and shielded tissues. Genome Biol **5:**R16

Casati P, Campi M, Chu F, Suzuki N, Maltby D, Guan S, Burlingame AL, Walbot V (2008) Histone acetylation and chromatin remodeling are required for UV-B dependent transcriptional activation of regulated genes in maize. Plant Cell **20:** 827-842

Castellano MM, del Pozo JC, Ramirez-Parra E, Brown S, Gutierrez C (2001) Expression and stability of arabidopsis CDC6 are associated with endoreplication. Plant Cell **13:** 2671–2686

Clough SJ, Bent AF (1998) Floral dip: a simplified method for Agrobacterium-mediated transformation of Arabidopsis thaliana. Plant J **16:**735-743

Desvoyes B, Ramirez-Parra E, Xie Q, Chua NH, Gutierrez C (2006) Cell type-specific role of the retinoblastoma/E2F pathway during Arabidopsis leaf development. Plant Physiol **140:** 67–80

Donham DC 2nd, Scorgie JK, Churchill ME (2011) The activity of the histone chaperone yeast Asf1 in the assembly and disassembly of histone H3/H4-DNA complexes. Nucleic Acids Res **39:** 5449-5458

Ehsan H, Reichheld JP, Durfee T, Roe JL (2004) TOUSLED kinase activity oscillates during the cell cycle and interacts with chromatin regulators. Plant Physiol **134:** 1488–1499

Eberharter A, Becker PB (2002) Histone acetylation: A switch between repressive and permissive chromatin. Second in review on chromatin dynamics. EMBO Rep **3:** 224-229

Franco AA, Lam WM, Burgers PM, Kaufman PD (2005) Histone deposition protein Asf1 maintains DNA replisome integrity and interacts with replication factor C. Genes Dev **19:** 1365–1375

Friedberg EC, Walker GC, Siede W (1995) DNA damage. Washington, DC: *ASM Press*

Gallagher TF, Ellis RJ (1982) Light-stimulated transcription of genes for two chloroplast polypeptides in isolated pea leaf nuclei. EMBO J **1:**1493-1498

Hennig L, Menges M, Murray JA, Gruissem W (2003) Arabidopsis transcript profiling on Affymetrix GeneChip arrays. Plant Mol Biol **53:**457-465

Jansen MAK, Gaba V, Greenberg BM (1998) Higher plants and UV-B radiation: balancing damage, repair and acclimation. Trends Plant Sci **3:** 131–135

Gutierrez C, Ramirez-Parra E, Castellano MM, Del Pozo JC (2002) G1 to S transition: more than a cell cycle engine switch. Curr Opin Plant Biol **5:** 480–486

Hayashi R, Goto Y, Tanaka R, Oonogi K, Hisasue M, Yoshida K (2007) Transcriptional regulation of human chromatin assembly factor ASF1. DNA Cell Biol **26:** 91-99

Hays JB (2002) Arabidopsis thaliana, a versatile model system for study of eukaryotic genome-maintenance functions. DNA Repair **1:** 579-600

Jefferson RA, Kavanagh TA, Bevan MW (1987) GUS fusions: B-glucuronidase as a sensitive and versatile gene fusion marker in higher plants. EMBO J **6:** 3901-3907

Jiao Y, Seeger K, Lautrette A, Gaubert A, Mousson F, Guerois R, Mann C, Ochsenbein F (2012) Surprising complexity of the Asf1 histone chaperone-Rad53 kinase interaction. Proc Natl Acad Sci USA **109:** 2866–2871

Kimura S, Sakaguchi K (2006) DNA Repair in Plants. Chem Rev **106:** 753-766

Lammens T, Boudolf V, Kheibarshekan L, Zalmas LP, Gaamouche T, Maes S, Vanstraelen M, Kondorosi E, La Thangue NB, Govaerts W., et al (2008) Atypical E2F activity restrains APC/$C^{CCS52A2}$ function obligatory for endocycle onset. Proc Natl Acad Sci USA **105:** 14721–14726

Lario LD, Ramirez-Parra E, Gutierrez C, Casati P, Spampinato CP (2011) Regulation of plant MSH2 and MSH6 genes in the UV-B-induced DNA damage response. J Exp Bot **62:** 2925–2937

Le S, Davis C, Konopka JB, Sternglanz R (1997) Two new S-phase-specific genes from *Saccharomyces cerevisiae*. Yeast **13:** 1029–1042

Lincker F, Roa H, Lang J, Sanchez-Calderon L, Smetana O, Cognat V, Keller M, Mediouni C, Houlne G, Chaboute ME (2008) Plant E2F factors in cell cycle, development and DNA damage response. India: Research Signpost

Mariconti L, Pellegrini B, Cantoni R, Stevens R, Bergounioux C, Cella R, Albani D (2002) The E2F family of transcription factors from Arabidopsis thaliana. Novel and conserved components of the retinoblastoma/E2F pathway in plants. J Biol Chem **277:** 9911-9919

Masumoto H, Hawke D, Kobayashi R, Verreault A (2005). A role for cell-cycle-regulated histone H3 lysine 56 acetylation in the DNA damage response. Nature **436:** 294–298

Mazza CA, Boccalandro HE, Giordano CV, Battista D, Scopel AL, Ballaré CL (2000) Functional significance and induction by solar radiation of ultraviolet-absorbing sunscreens in field-grown soybean crops. Plant Physiol **122:** 117-125

Minard LV, Williams JS, Walker AC, Schultz MC (2011) Transcriptional Regulation by Asf1. New mechanistic insights from studies of the DNA damage response to replication stress. J Biol Chem **286:** 7082–7092

Myung K, Pennaneach V, Kats ES, Kolodner RD (2003) *Saccharomyces cerevisiae* chromatin-assembly factors that act during DNA replication function in the maintenance of genome stability. Proc Natl Acad Sci USA **100:** 6640–6645

Naouar N, Vandepoele K, Lammens T, Casneuf T, Zeller G, van Hummelen P, Weigel D, Ratsch G, Inze D, Kuiper M, De Veylder L, Vuylsteke M (2009) Quantitative RNA expression analysis with Affymetrix Tiling 1.0R arrays identifies new E2F target genes. Plant J **57:** 184–194

Osada S, Sutton A, Muster N, Brown CE., Yates III JR, Sternglanz R, Workman JL (2001)The yeast SAS (something about silencing) protein complex contains a MYST-type putative acetyltransferase and functions with chromatin assembly factor ASF1. Genes Dev **15:** 3155–3168

Pandey R, Mueller A, Napoli CA, Selinger DA, Pikaard CS, Richards EJ, Bender J, Mount DW, Jorgensen RA (2002) Analysis of histone acetyltransferase and histone deacetylase families of Arabidopsis thaliana suggests functional diversification of chromatin modification among multicellular eukaryotes. Nucl Acids Res **30:** 5036-5055

Park YJ, Luger K (2008) Histone chaperones in nucleosome eviction and histone exchange. Curr Opin Struct Biol **18:** 282–289

Pfluger J, Wagner D (2007) Histone modifications and dynamic regulation of genome accessibility in plants. Curr Opin Plant Biol **10:** 645–652

Prado F, Cortes-Ledesma F, Aguilera A (2004) The absence of the yeast chromatin assembly factor Asf1 increases genomic instability and sister chromatid exchange. EMBO Rep **5:** 497–502

Qüesta JL, Walbot V, Casati P (2010) Mutator transposon activation after UV-B involves chromatin remodeling and DNA demethylation. Epigenetics **5:** 352-363

Ramey CJ, Howar S, Adkins M, Linger J, Spicer J, Tyler JK (2004) Activation of the DNA damage checkpoint in yeast lacking the histone chaperone antisilencing function 1. Mol Cell Biol **24:** 10313–10327

Ramirez-Parra E, Gutierrez C (2000) Characterization of wheat DP, a heterodimerization partner of the plant E2F transcription factor which stimulates E2F–DNA binding. FEBS Lett **486:** 73–78

Ramirez-Parra E, Lopez-Matas MA, Frundt C, Gutierrez C (2004) Role of an atypical E2F transcription factor in the control of Arabidopsis cell growth and differentiation. Plant Cell **16**: 2350–2363

Ramirez-Parra E, Gutierrez C (2007). E2F regulates FASCIATA1, a chromatin assembly gene whose loss switches on the endocycle and activates gene expression by changing the epigenetic status. Plant Physiol **144:** 105–120

Rozen S, Skaletsky H (2000) Primer3 on the WWW for general users and for biologist programmers. Methods Mol Biol **132:** 365–386

Sapountzi,V; Logan, IR; Robson CN (2006) Cellular functions of TIP60. Int J Biochem Cell Biol **38:** 1496-1509

Sen S, De Benedetti A (2006) TLK1B promotes repair of UV-damaged DNA through chromatin remodeling by Asf1. BMC Mol Biol **7:**37

Schulz LL, Tyler JK (2006) The histone chaperone ASF1 localizes to active DNA replication forks to mediate efficient DNA replication. FASEB J **20:** 488–490

Shen W-H (2002) The plant E2F–Rb pathway and epigenetic control. Trends Plant Sci **7:** 505–511

Singer MS, Kahana A, Wolf AJ, Meisinger LL, Peterson SE, Goggin C, Mahowald M, Gottschling DE (1998) Identification of high-copy disruptors of telomeric silencing in *Saccharomyces cerevisiae*. Genetics **150:** 613–632

Squatrito M, Gorrini C, Amati B (2006) Tip60 in DNA damage response and growth control: many tricks in one HAT. Trends Cell Biol **16:** 433-442

Stevens R, Mariconti L, Rossignol P, Perennes C, Cella R, Bergounioux C (2002) Two E2F sites in the Arabidopsis MCM3 promoter have different roles in cell cycle activation and meristematic expression.J Biol Chem **277:** 32978-32984

Sun Y, Jiang X, Price BD (2010) Tip60 Connecting chromatin to DNA damage signaling. Cell Cycle **9:** 930-936

Tagami H, Ray-Gallet D, Almouzni G, Nakatani Y (2004) Histone H3.1 and H3.3 complexes mediate nucleosome assembly pathways dependent or independent of DNA synthesis. Cell **116:** 51–61

Tang Y, Poustovoitov MV, Zhao K, Garfinkel M, Canutescu A, Dunbrack R, Adams PD, Marmorstein R (2006) Structure of a human ASF1a-HIRA complex and insights into specificity of histone chaperone complex assembly. Nat Struct Mol Biol **13:** 921–929

Tyler JK, Adams CR, Chen SR, Kobayashi R, Kamakaka RT, Kadonaga JT (1999) The RCAF complex mediates chromatin assembly during DNA replication and repair. Nature 402: 555–560

Ulm R, Baumann A, Oravecz A, Mate Z, Adam E, Oakeley EJ, Schafer E, Nagy F (2004) Genome-wide analysis of gene expression reveals function of the bZIP transcription factor HY5 in the UV-B response of Arabidopsis. Proc Natl Acad Sci USA **101:** 1397–1402

Vaillant I, Paszkowski J (2007) Role of histone and DNA methylation in gene regulation. Curr Opin Plant Biol **10:** 528–533

Vandepoele K, Vlieghe K, Florquin K, Hennig L, Beemster GTS, Gruissem W, Van De Peer Y, Inzé D, De Veylder L (2005) Genome-wide identification of potential plant E2F target genes. Plant Physiol **139:** 316–328

Verbsky ML, Richards EJ (2001) Chromatin remodeling in plants. Curr Opin Plant Biol **4:** 494–500

Wang Y, Liu J, Xia R, Wang J, Shen J, Cao R, Hong X, Zhu J-K, Gong Z (2007) The protein kinase TOUSLED is required for maintenance of transcriptional gene silencing in Arabidopsis. EMBO Rep **8:** 77-83

Xu F, Zhang K, Grunstein M (2005) Acetylation in histone H3 globular domain regulates gene expression in yeast. Cell **121:** 375–385

Yamane K, Mizuguchi T, Cui B, Zofall M., Noma K, Grewal SIS (2011) Asf1/HIRA Facilitate Global Histone Deacetylation and Associate with HP1 to Promote Nucleosome Occupancy at Heterochromatic Loci. Mol Cell **41:** 56–66

Yuan G, Zhu B (2012) Histone variants and epigenetic inheritance. Biochim Biophys Acta **1819:** 222–229

Zhang R, Poustovoitov MV, Ye X, Santos HA, Chen W, Daganzo SM, Erzberger JP, Serebriiskii IG, Canutescu AA, Dunbrack RL, Pehrson JR, Berger JM, Kaufman PD, Adams PD (2005) Formation of MacroH2A-containing senescence-associated heterochromatin foci and senescence driven by ASF1a and HIRA. Dev Cell **8:** 19–30

Zhu Y, Weng M, Yang Y, Zhang C, Li Z, Shen WH, Dong A (2011) Arabidopsis homologues of the histone chaperone ASF1 are crucial for chromatin replication and cell proliferation in plant development. Plant J **66:** 443–455

Zhu Y, Dong A, Shen W-H (2012) Histone variants and chromatin assembly in plant abiotic stress responses. Biochim Biophys Acta **1819:** 343-348

Figure legends

Figure 1. Histochemical localization of GUS activity in transgenic plants carrying the *ASF1A* (A-G) and *ASF1B* (H-Q) promoters. Panel A: 3-d-old whole seedlings. Panel H: 6-d-old whole seedlings. Panels B and K: roots from 10-d-old seedlings. Panels C and I: 10-d-old wild-type whole seedlings. Panel J: magnification of panel I. Panel D: proliferating leaves. Panels E and L: mature leaves. Panels F and Q: siliques. Panel Q: magnification of panel P. Panels G, M and O: flowers at different stages of development. Panel N: magnification of panel M.

Figure 2. E2F *in vitro* binding to *ASF1A* and *ASF1B* proximal promoters. A, Scheme of the *ASF1A* and *ASF1B* proximal promoters showing the position and sequence of E2F-binding sites. B-D, Electrophoretic mobility shift assay analysis of protein–DNA complexes performed with recombinant E2Fa/Dpa, E2Fe, and E2Ff proteins and a fragment of the promoter containing the E2F sites as a probe: B, site at -330 bp from the ATG translation start codon of the *ASF1A* promoter; C, site at -138 bp from the ATG translation start codon of the *ASF1B* promoter; D, site at -276 bp from the ATG translation start codon of the *ASF1B* promoter. Lane 1, free probe; lanes 2–4, binding of E2Fa/Dpa, E2Fe, or E2Ff, respectively, to the promoter; lanes 5–7, protein–DNA complexes were competed out with a 100-fold molar excess of unlabelled oligonucleotide containing a consensus E2F site (WT); lanes 8–10, specific protein–DNA binding was challenged with a 100-fold molar excess of a mutated oligonucleotide (Mut).

Figure 3. E2F-regulated expression of *ASF1A* and *ASF1B* genes. A, Expression levels of *ASF1A, ASF1B* and *CDC6* genes determined by RT-qPCR analysis in transgenic plants overexpressing each of the six Arabidopsis E2F transcription factors ($E2F^{OE}$). Measurements are relative to the amount in WT plants. Asterisks indicate statistical differences applying the Student's t-test ($P < 0.05$). B, Relative expression levels of *ASF1A, ASF1B* and *CDC6* genes determined by RT-qPCR analysis in transgenic plants overexpressing RepA protein compared with plants overexpressing RepA-E198K protein. C, ChIP assays using antibodies anti-myc or anti-HA with nuclei prepared from WT or transgenic plants expressing *myc-E2Fd*, *HA-E2Fe* or *HA-E2Ff*. The immunoprecipitates and input DNA before immunoprecipitation were analyzed by PCR for the presence of promoter sequences of *ASF1A* and *ASF1B*; *ACT2*, a control gene that is not regulated by E2F factors; and *MCM3*, a control gene that is regulated by E2F factors. Three PCR experiments were done with each sample.

Figure 4. Relative transcript levels of Arabidopsis *ASF1A* (A) and *ASF1B* (B) measured by RT-qPCR in wild-type plants (Ws-2) and in *asf1a*/*asf1b* RNAi transgenic plants (lines CS3995, CS3996 and CS30921). C and D, Comparison of the rosette area in wild-type and *asf1a*/*asf1b* RNAi transgenic

plants from 16-19 days after sown (DAS). Asterisks indicate the statistical differences applying the Student's t-test ($P < 0.05$).

Figure 5. A, Western blot analysis using anti-ASF1 antibodies and *E. coli* protein extracts expressing GST-ASF1A fusion protein (+). As a control, an *E. coli* protein extract before induction was used (-). B and C, Coimmunoprecipitation experiments using anti-ASF1 (B) or anti-HAM (C) antibodies. As a control, a nuclei protein extract not incubated with any antibody was used (-).Western blots were developed using antibodies anti-N-terminal acetylated H3 (Ac H3) or H4 (Ac H4) or anti-TIP60 (HAM1/HAM2). Prestained molecular weight markers (MWM) and their corresponding molecular mass are included at the right side of each gel.

Figure 6. UV-B-regulated expression of *ASF1A* and *ASF1B* genes. Relative expression levels of *ASF1A* (A) and *ASF1B* (B) were determined by RT-qPCR analysis. Arabidopsis seedlings of 11, 16, 19 and 28 DAS were irradiated with a 4h-UV-B treatment (UV-B), or kept under control conditions without UV-B. Each reaction was normalized using the cycle threshold (Ct) values corresponding to the *CPK3* transcript, which is not regulated by UV-B. Asterisks indicate the statistical differences applying Student's t-test ($P < 0.05$). C, ChIP assays performed using antibodies anti-N-terminal acetylated H3 (Ac H3) or H4 (Ac H4) and nuclei prepared from WT seedlings after a 4h-UV-B treatment (UV-B), or kept under control conditions without UV-B. Immunoprecipitated and input DNA before immunoprecipitation were analyzed for the presence of *ASF1A* and *ASF1B* promoter sequences. Three PCR experiments were carried out with each sample. Asterisks indicate statistical differences applying the Student's t-test ($P < 0.05$). D, UV-B-regulated expression of the *E2F* genes. WT plants were irradiated with UV-B light for 4h (UV-B) or kept under control conditions as indicated in Materials and Methods. Expression levels of UV-B irradiated vs control samples were determined by RT-qPCR analysis. Data show mean values ± S.D. of at least three independent experiments. Asterisks indicate statistical differences applying the Student's t-test ($P < 0.05$). E, CPD levels in the DNA of WT and *asf1a/asf1b* RNAi transgenic seedlings (CS3995 line) under control conditions without UV-B (control), immediately after or 2 h later a 4h-UV-B treatment (UV-B). Experiments were done under conditions that allowed photorepair in the light (light), or under dark conditions (dark). CPD levels are indicated as integrated optical density (IOD) values. Results represent the average ± S.E.M. of three independent biological replicates. F, Relative expression of *UVR2, UVR3* and *UVR7* transcripts by RT-qPCR. WT and *asf1a/asf1b* RNAi transgenic (CS3995 line) seedlings were irradiated with UV-B for 4 h (UV-B) or were kept under control conditions without UV-B (control). Data show mean values ± S.D. of at least three independent experiments. For each transcript analyzed, different letters indicate significant statistical difference ($P < 0.05$).

Supplemental Figures and Table Legends

Supplemental Figure S1. Cell cycle regulated expression of genes encoding *ASF1A* and *ASF1B*. Data were obtained with Arabidopsis cultured cells synchronized by sucrose starvation for 24 h. Samples were prepared at the indicated times (in hours) after release from the sucrose block and processed for microarray experiments. Data were collected from publicly available collection of microarray data and have been generated using the Genevestigator© tool package. Gene expression levels have been made relative to the value at the time of sucrose starvation release (T=0 h). The pattern of *MCM3* and cyclin *CYCB1;4* expression has been included as a reference for well-characterized genes up-regulated at the G1/S or G2/M transition, respectively and *ACT2* that remains constant during the cell cycle.

Supplemental Figure S2. Histochemical localization of GUS activity in transgenic plants carrying the *ASF1A* (*pASF1A:GUS*) and *ASF1B* (*pASF1B:GUS*) promoters in control plants in the absence of UV-B, and after 4h of UV-B radiation.

Supplemental Table SI. *Gene-specific oligonucleotides used for EMSA assays*

Supplemental Table SII. *Gene-specific oligonucleotides used for RT-qPCR*

Supplemental Table SIII. *Gene-specific oligonucleotides used for ChIP assays*

Supplemental Table SIV. *Gene-specific oligonucleotides used for GUS assay*

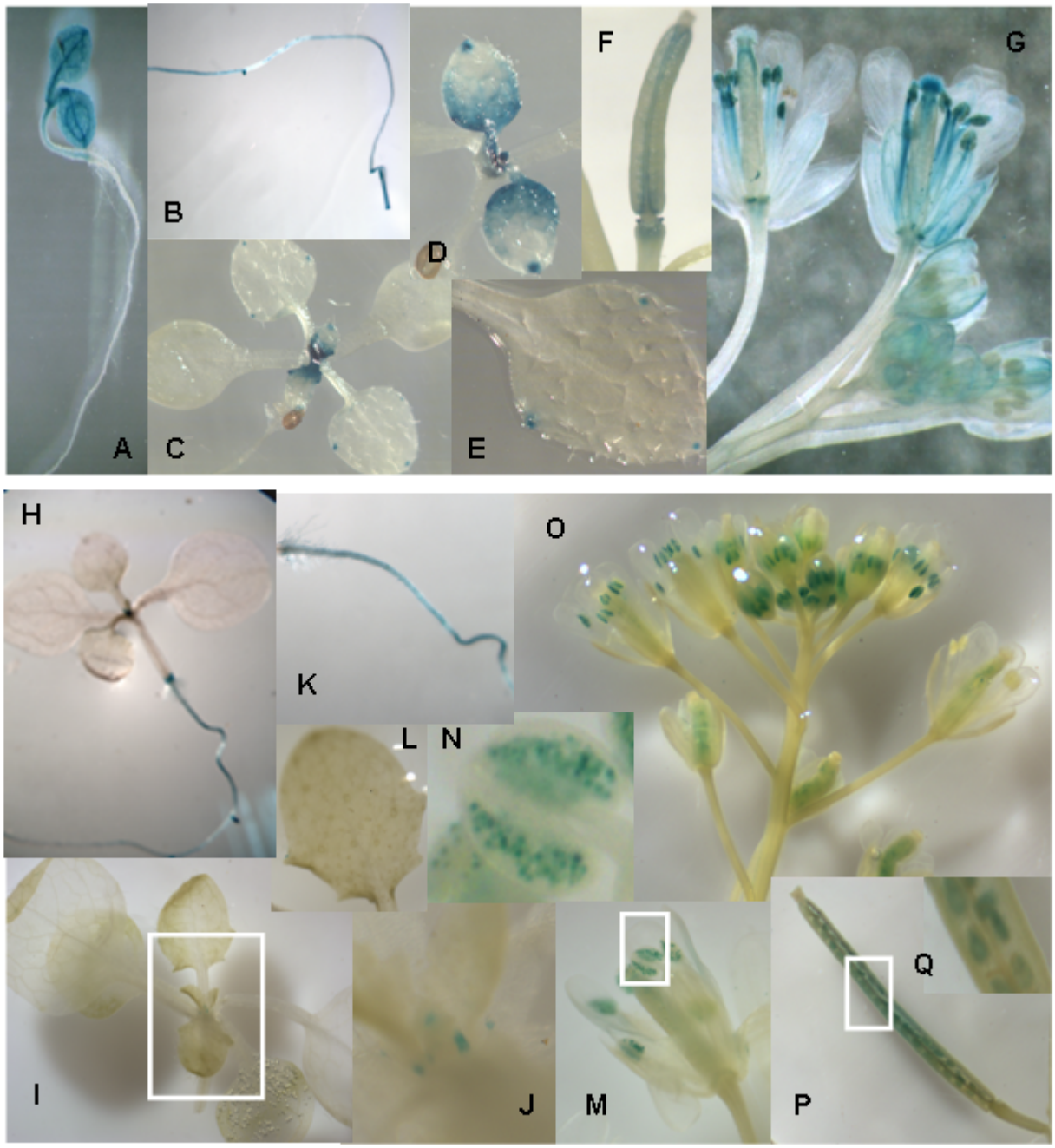

Figure 1. Histochemical localization of GUS activity in transgenic plants carrying the ASF1A (A-G) and ASF1B (H-Q) promoters. Panels A and H: 3-d-old whole seedlings. Panels B and K: roots from 10-d-old seedlings. Panels C and I: 10-d-old wild-type whole seedlings. Panel J: magnification of panel I. Panel D: proliferating leaves. Panels E and L: mature leaves. Panels F and Q: siliques. Panel Q: magnification of panel P. Panels G, M and O: flowers at different stages of development. Panel N: magnification of panel M.

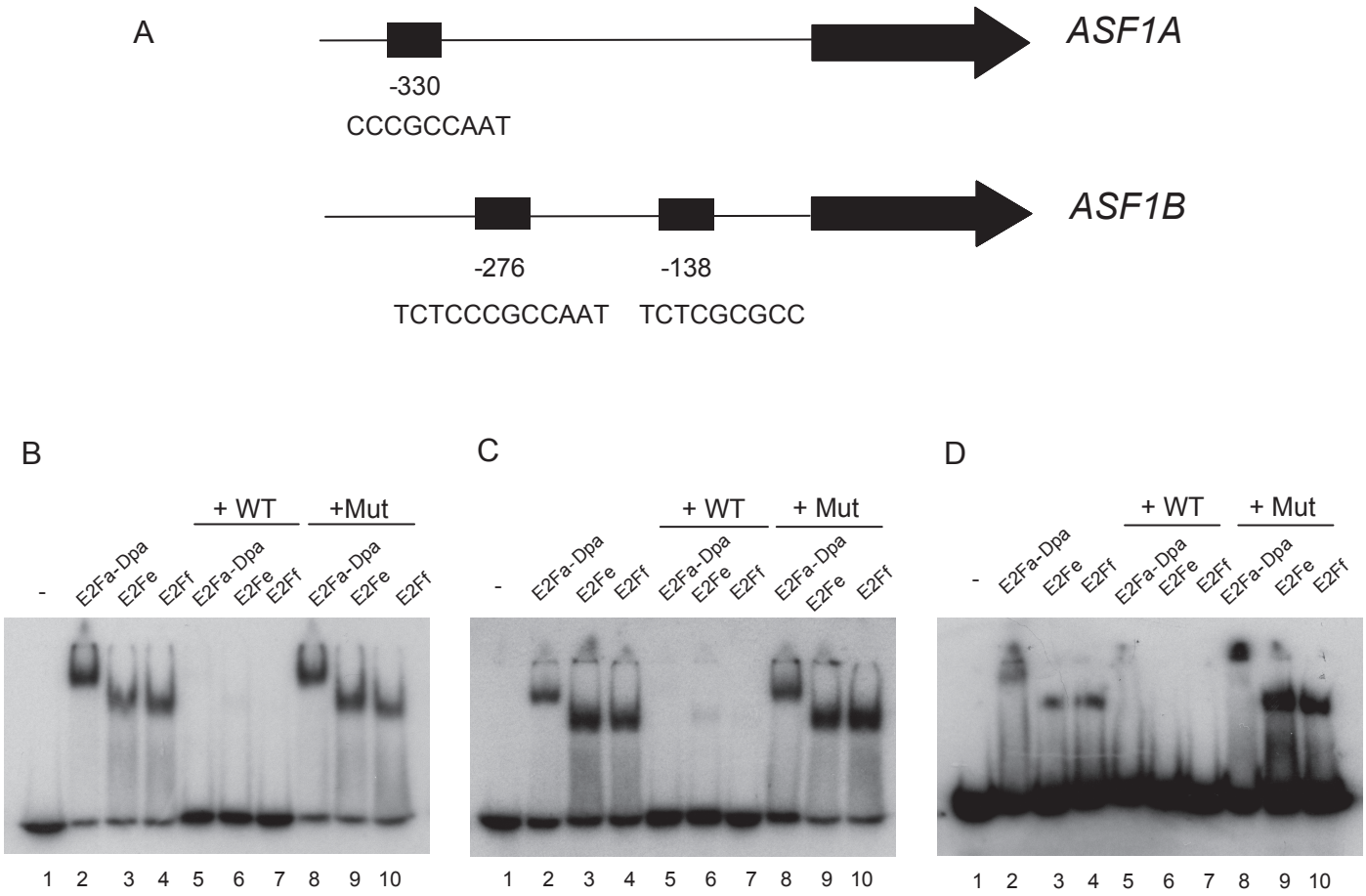

Figure 2. E2F in vitro binding to ASF1A and ASF1B proximal promoters. A, Scheme of the ASF1A and ASF1B proximal promoters showing the position and sequence of E2F-binding sites. B-D, Electrophoretic mobility shift assay analysis of protein–DNA complexes performed with recombinant E2Fa/Dpa, E2Fe, and E2Ff proteins and a fragment of the promoter containing the E2F sites as a probe: B, site at -330 bp from the ATG translation start codon of the ASF1A promoter; C, site at -138 bp from the ATG translation start codon of the ASF1B promoter; D, site at -276 bp from the ATG translation start codon of the ASF1B promoter. Lane 1, free probe; lanes 2–4, binding of E2Fa/Dpa, E2Fe, or E2Ff, respectively, to the promoter; lanes 5–7, protein–DNA complexes were competed out with a 100-fold molar excess of unlabelled oligonucleotide containing a consensus E2F site (WT); lanes 8–10, specific protein–DNA binding was challenged with a 100-fold molar excess of a mutated oligonucleotide (Mut).

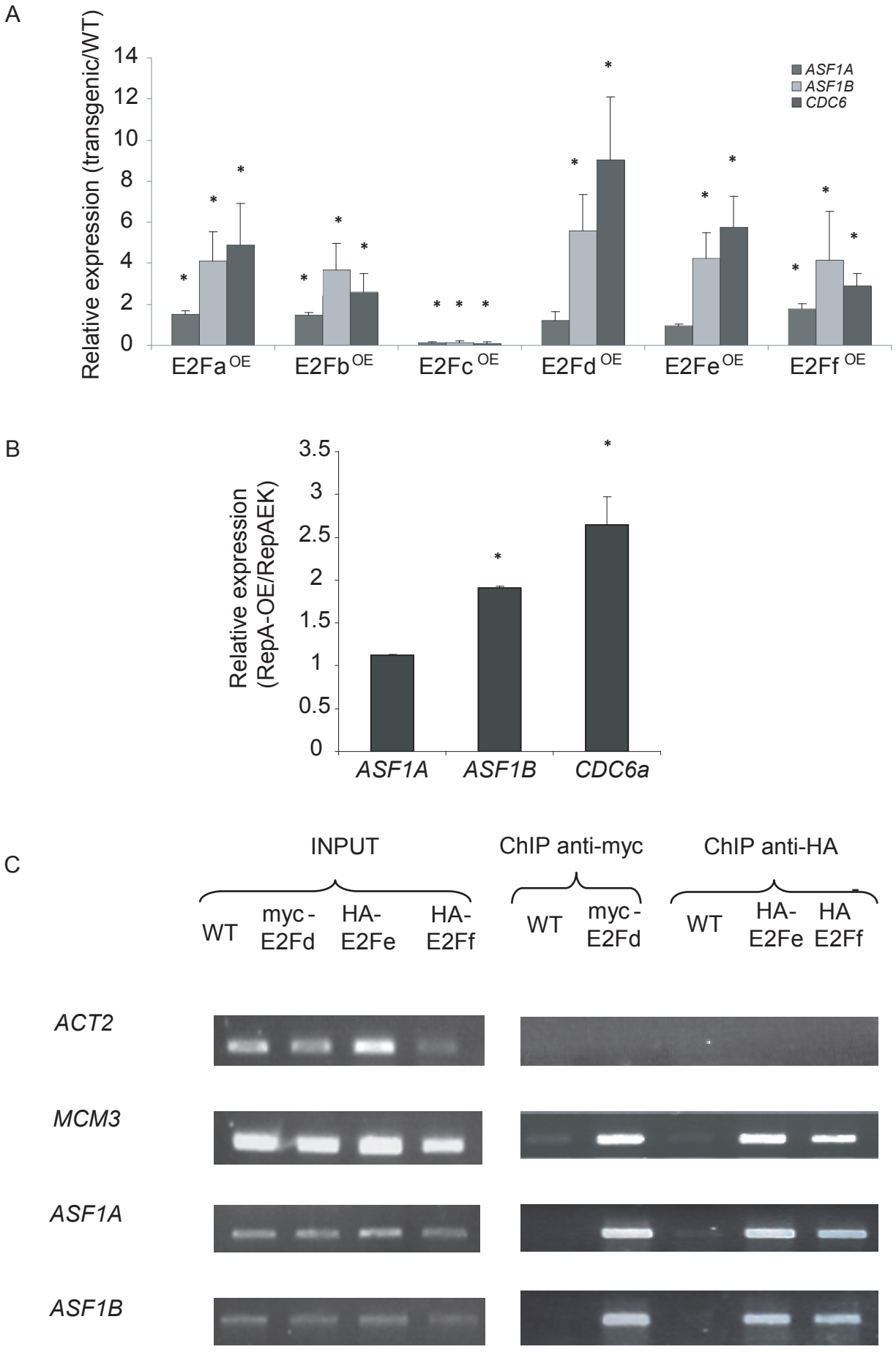

Figure 3. E2F-regulated expression of ASF1A and ASF1B genes. A, Expression levels of ASF1A, ASF1B and CDC6a genes determined by RT-qPCR analysis in transgenic plants overexpressing each of the six Arabidopsis E2F transcription factors (E2FOE). Measurements are relative to the amount in WT plants. Asterisks indicate statistical differences applying the Student's t-test ($P < 0.05$). B, Relative expression levels of ASF1A, ASF1B and CDC6 genes determined by RT-qPCR analysis in transgenic plants overexpressing RepA protein compared with plants overexpressing RepA-E198K protein. C, ChIP assays using antibodies anti-myc or anti-HA with nuclei prepared from WT or transgenic plants expressing myc-E2Fd, HA-E2Fe or HA-E2Ff. The immunoprecipitates and input DNA before immunoprecipitation were analyzed by PCR for the presence of promoter sequences of ASF1A and ASF1B; ACT2, a control gene that is not regulated by E2F factors; and MCM3, a control gene that is regulated by E2F factors. Three PCR experiments were done with each sample.

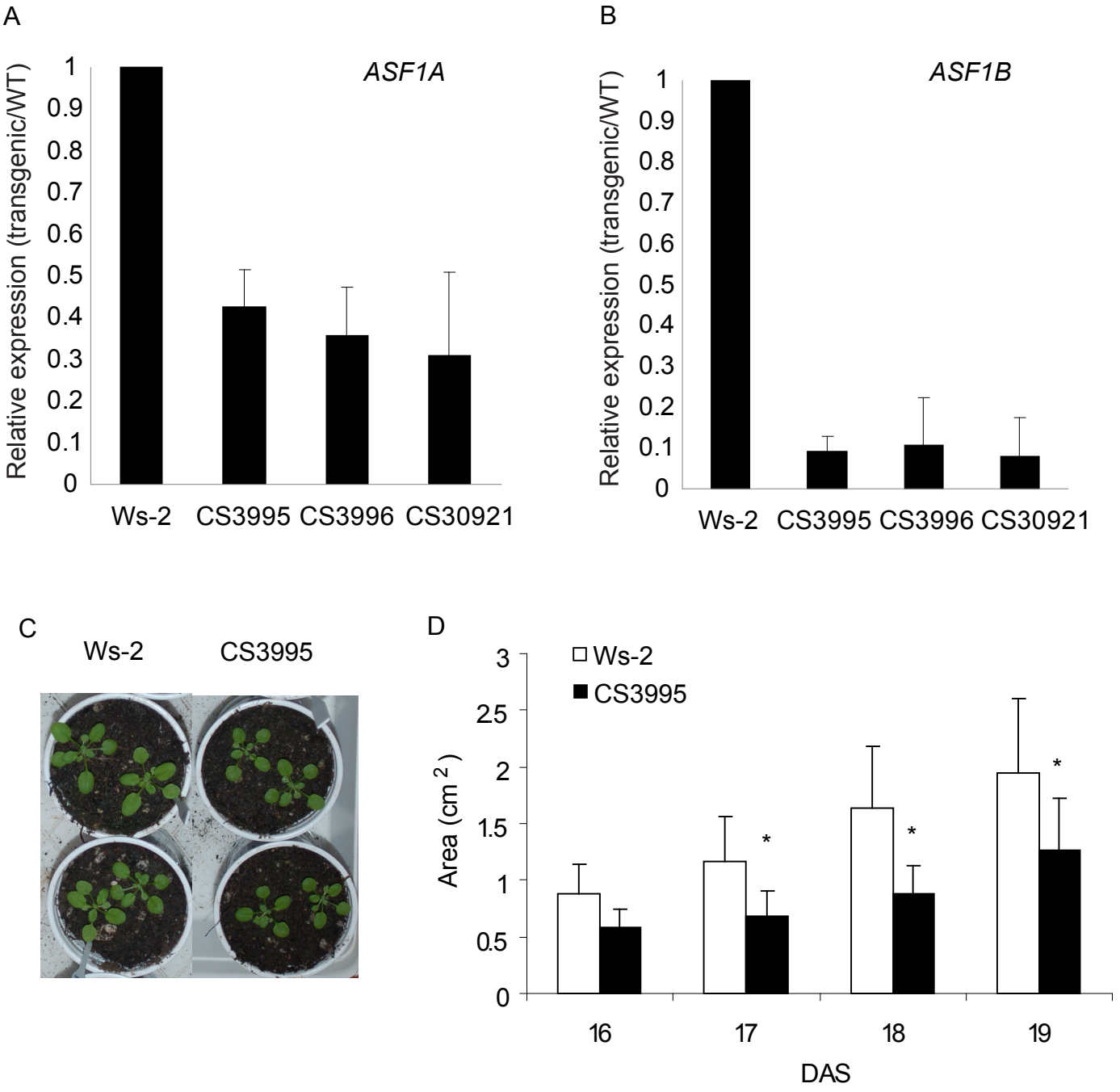

Figure 4. Relative transcript levels of Arabidopsis ASF1A (A) and ASF1B (B) measured by RT-qPCR in wild-type plants (Ws-2) and in asf1a/asf1b RNAi transgenic plants (lines CS3995, CS3996 and CS30921). C and D, Comparison of the rosette area in wild-type and asf1a/asf1b RNAi transgenic plants from 16-19 days after sown (DAS). Asterisks indicate the statistical differences applying the Student's t-test ($P < 0.05$).

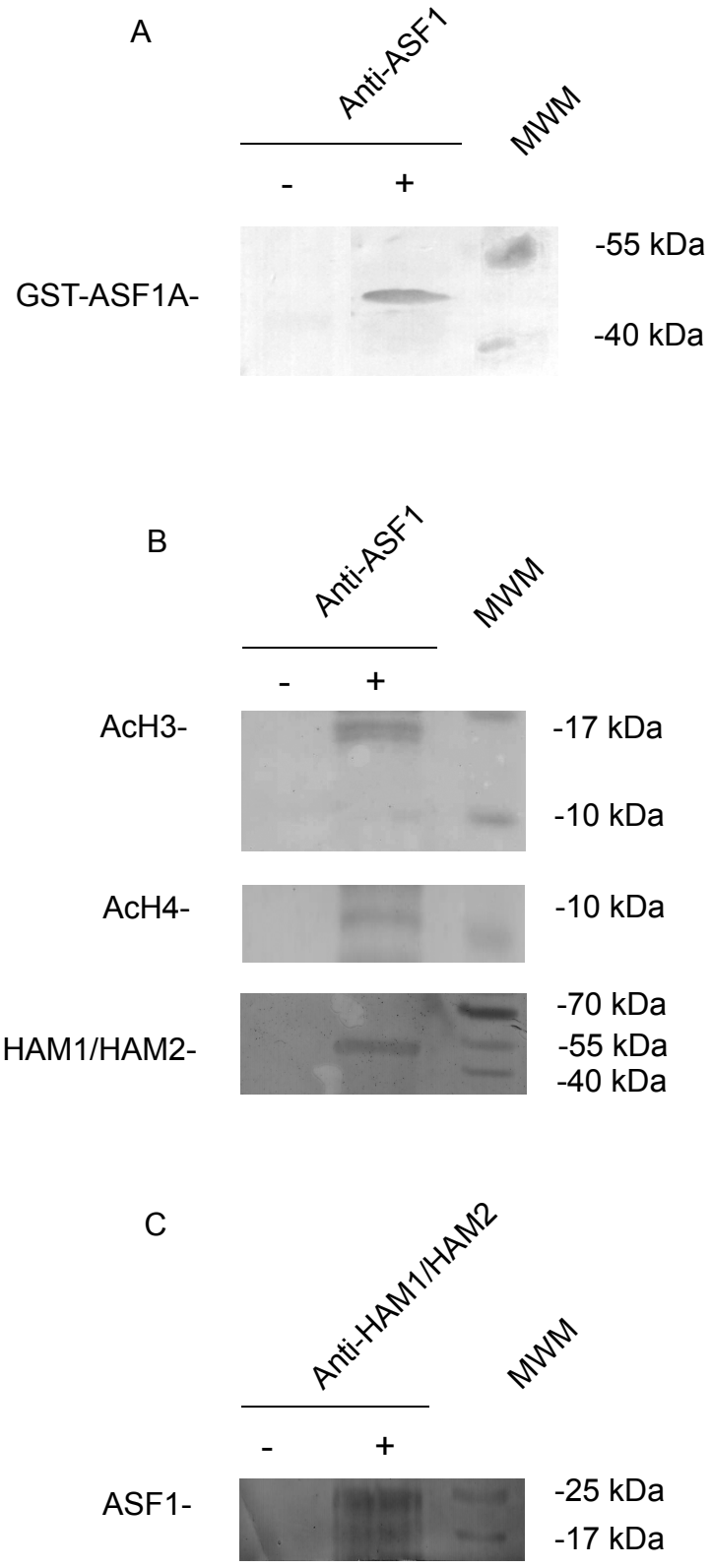

Figure 5. A, Western blot analysis using anti-ASF1 antibodies and E. coli protein extracts expressing GST-ASF1A fusion protein (+). As a control, a E.coli protein extract before induction was used (-). B and C, Coimmunoprecipitation experiments using anti-ASF1 (B) or anti-TIP60 (C) antibodies. As a control, a nuclei protein extract not incubated with any antibody was used (-).Western blots were developed using antibodies anti-N-terminal acetylated H3 (Ac H3) or H4 (Ac H4) and anti-TIP60 (HAM1/HAM2). Prestained MWM and their corresponding molecular mass are included at the right side of each gel.

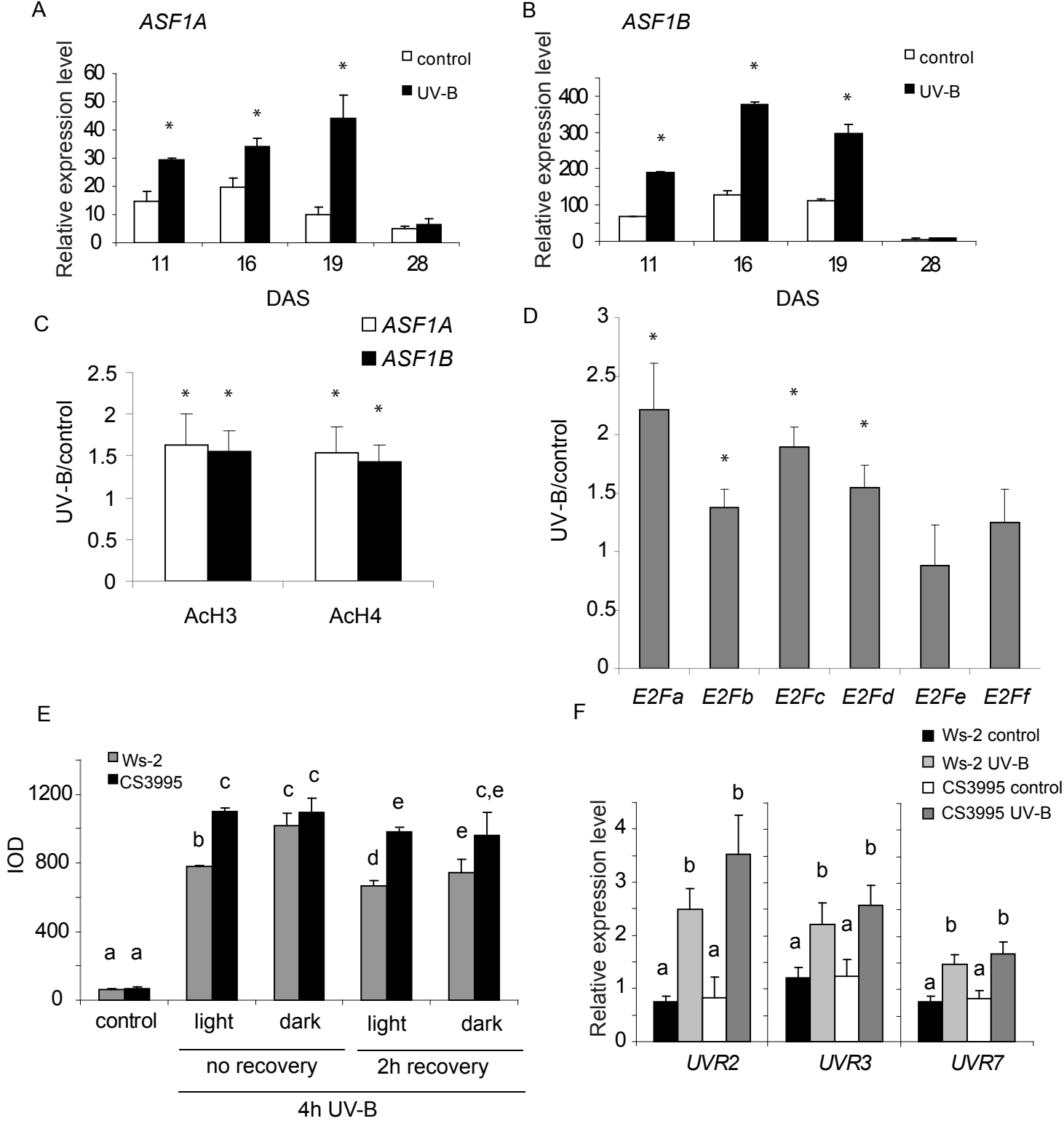

Figure 6. UV-B-regulated expression of ASF1A and ASF1B genes. Relative expression levels of ASF1A (A) and ASF1B (B) were determined by RT-qPCR analysis. Arabidopsis seedlings of 11, 16, 19 and 28 DAS were irradiated with a 4h-UV-B treatment (UV-B), or kept under control conditions without UV-B. Each reaction was normalized using the cycle threshold (Ct) values corresponding to the CPK3 transcript, which is not regulated by UV-B. Asterisks indicate the statistical differences applying Student's t-test ($P < 0.05$). C, ChIP assays performed using antibodies anti-N-terminal acetylated H3 (Ac H3) or H4 (Ac H4) and nuclei prepared from WT seedlings after a 4h-UV-B treatment (UV-B), or kept under control conditions without UV-B. Immunoprecipitated and input DNA before immunoprecipitation were analyzed for the presence of ASF1A and ASF1B promoter sequences. Three PCR experiments were carried out with each sample. Asterisks indicate statistical differences applying the Student's t-test ($P < 0.05$). D, UV-B-regulated expression of the E2F genes. WT plants were irradiated with UV-B light for 4h (UV-B) or kept under control conditions as indicated in Materials and Methods. Expression levels of UV-B irradiated vs control samples were determined by RT-qPCR analysis. Data show mean values ± S.D. of at least three independent experiments. Asterisks indicate statistical differences applying the Student's t-test ($P < 0.05$). E, CPD levels in the DNA of WT and asf1a/asf1b RNAi transgenic seedlings (CS3995 line) under control conditions without UV-B (control), immediately after or 2 h later a 4h-UV-B treatment (UV-B). Experiments were done under conditions that allowed photorepair in the light (light), or under dark conditions (dark). CPD levels are indicated as integrated optical density (IOD) values. Results represent the average ± S.E.M. of three independent biological replicates. F, Relative expression of UVR2, UVR3 and UVR7 transcripts by RT-qPCR. WT and asf1a/asf1b RNAi transgenic (CS3995 line) seedlings were irradiated with UV-B for 4 h (UV-B) or were kept under control conditions without UV-B (control). Data show mean values ± S.D. of at least three independent experiments. For each transcript analyzed, different letters indicate significant statistical difference ($P < 0.05$).